Surface plasmon polariton mediated energy transfer from external antennas into organic photovoltaic cells

by

Timothy David Heidel

S.B., E.E. M.I.T., 2005

Submitted to the Department of Electrical Engineering and Computer Science
in partial fulfillment of the requirements for the degree of

Master of Engineering in Electrical Engineering and Computer Science

at the

MASSACHUSETTS INSTITUTE OF TECHNOLOGY

September 2006

Author .....
Department of Electrical Engineering and Computer Science
August 22, 2006

Certified by .....
Marc A. Baldo
Associate Professor
Thesis Supervisor

Accepted by .....
Arthur C. Smith
Professor of Electrical Engineering
Chairman, Department Committee on Graduate Theses

Surface plasmon polariton mediated energy transfer from external antennas into organic photovoltaic cells

by

Timothy David Heidel

Submitted to the Department of Electrical Engineering and Computer Science
on August 22, 2006, in partial fulfillment of the
requirements for the degree of
Master of Engineering in Electrical Engineering and Computer Science

Abstract

Despite significant improvements in the performance of organic photovoltaic devices in recent years, the tradeoff between light absorption and charge separation efficiency remains pervasive; increasing light absorption by increasing the device thickness leads to a decrease in exciton diffusion efficiency and vice versa.

In this thesis, I demonstrate organic solar cells with an external light absorbing antenna. Light is absorbed by the external antenna and subsequently transferred into the photovoltaic cell via surface plasmon polariton modes in an interfacial thin silver contact. By decoupling the optical and electrical functions of the cell, this new architecture has the potential to circumvent the tradeoff between light absorption and charge separation efficiency. Non-radiative energy transfer is discussed and modeling finds that efficient energy transfer is mediated by surface plasmon polaritons.

Devices with two very different antenna systems are demonstrated experimentally. Antennas with high photoluminesence efficiency are found to exhibit energy transfer efficiencies of approximately 50% while strongly absorbing antennas exhibit increases in photocurrent as high as 700% when compared to devices with non-functioning antennas even with very low photoluminesence efficiencies near 4%.

These results suggest that this new device architecture could lead to significantly higher power conversion efficiencies by allowing the independent optimization of the optical and electrical components of organic photovoltaic cells.

Thesis Supervisor: Marc A. Baldo
Title: Associate Professor

Acknowledgments

First and foremost, I must thank my research supervisor, Marc Baldo, for his unceasing guidance and support of both this research and my own continuing development as a student and researcher.

I am also indebted to the other members of the Soft Semiconductor Group whose efforts, results, and ideas have influenced that which is presented here including: Jon Mapel, Kemal Celebi, Mike Currie, Madhusudan Singh, Michael Segal, Mihai Bora, and Kaveh Milaninia. Jon, especially, deserves thanks for serving as an extraordinary colleague, mentor, and friend who has helped immeasurably in my transition into graduate school. I also owe thanks to Mihai for facilitating my initial introduction to the group and this field.

My family also deserves thanks. Their never-ending support and love has also played a large part in my successful pursuit of this milestone.

Contents

1 Introduction **11**

2 Organic Photovoltaics **13**

2.1 Mechanism of Power Conversion 13

2.2 Light Absorption vs. Charge Separation 16

2.3 Architectures Employed to Improve Efficiency 16

2.3.1 Bulk Heterojunction Cells 16

2.3.2 Dye-Sensitized Nanostructured Oxide Cells 18

2.3.3 Tandem (Stacked) Cells 19

2.4 Light Trapping Strategies 20

2.4.1 Optical Modeling 20

2.4.2 Diffraction Gratings and Buried Nanoelectrodes 22

2.4.3 Metal Nanoclusters 23

3 A Device Architecture Inspired by Photosynthesis **25**

3.1 Energy Transfer via Surface Plasmon Polariton Modes 26

3.2 Simulation of Energy Transfer Efficiency 30

3.3 Device Design Optimization 34

4 Demonstration of Organic PV with External Antennas **35**

4.1 Fabrication of Organic PV 35

4.2 Antenna Photoluminescence Efficiency 37

4.3 Current-Voltage Characteristics 38

4.4 Wavelength Resolved External Quantum Efficiency Detection 39
4.5 Calculation of Energy Transfer Efficiency 41

5 Conclusion **45**

List of Figures

2-1 Summary of power conversion processes in organic PV 14

2-2 Illustration of conduction in bulk heterojunction mixed semiconductor layers 17

2-3 Schematic illustration of the dye-sensitized nanostructured oxide cell architecture 19

2-4 Optical field modeling in organic PV 21

2-5 Schematic drawings of two light trapping architectures 22

3-1 Organic PV with an external antenna 26

3-2 Surface plasmon polariton orientation and field enhancement 27

3-3 Attenuated total reflection test setup and surface plasmon polariton dispersion relation 29

3-4 Exciton coupling fraction and mode profiles 32

3-5 Antenna energy transfer efficiency to organic layers 33

4-1 Structures of organic PV devices fabricated with antennas 37

4-2 Relative photoluminescence intensity 38

4-3 Current-voltage characteristics 39

4-4 Alq_3 antenna external quantum efficiency enhancement 41

4-5 $F_{20}TPP$ antenna external quantum efficiency enhancement 42

4-6 $F_{20}TPP$ antennas relative increase in external quantum efficiency . . 43

Chapter 1

Introduction

Despite significant improvements in the performance of photovoltaic (PV) devices in the past half-century, solar cells have yet to achieve widespread success as an alternative means of producing electricity.[1] Instead, the use of solar cells has been limited to specialized markets such as in satellites or for rural electrification.[2][3] In these applications, conventional electricity generation methods such as gas or coal burning power plants are often prohibitively expensive and impractical. On a cost per Watt generated basis, solar cells are simply too expensive for general use.[4]

Much of the past research into PV devices has borrowed expertise and fabrication techniques from the silicon microelectronics industry. Significant progress has been made in improving power conversion efficiencies with recent reports showing power conversion efficiencies as high as 24.4% for crystalline-silicon cells[5] and nearly 10% for amorphous silicon thin-film devices.[6][7] However, the energy intensive, high cost processes associated with inorganic semiconductor-based electronics fabrication have kept solar cells from competing successfully on the mass market.

Research into organic semiconductor based PVs, using small molecule pigments or polymers, has gained significant momentum in recent years as efficiencies have continued to rise steadily. The latest organic semiconductor based solar cells have exhibited power conversion efficiencies as high as 5.7%.[8] Organic semiconductor based devices have the potential for very low-cost production using techniques common in other industries such as roll-to-roll and web-based processing. Many of these techniques

are also well suited for making very large area devices. In addition, the variety of organic materials available (and the ability of chemists to continually synthesize new molecules for specialized applications) may also allow organic solar cells to match more innovative applications such as the design of solar cells directly into building windows. However, for any of these potential benefits to be realized the efficiency of organic PVs must be improved.

In this thesis, I demonstrate organic PV cells with an external light absorbing antenna. This concept was inspired by the physical architecture for photosynthesis found in plants and bacteria. By decoupling the optical and electrical functions, this new architecture has the potential to circumvent one of the most pervasive tradeoffs found in the design of organic PV cells: that between light absorption and charge separation efficiency. In these cells, light is absorbed by the external antenna and subsequently transferred into the photovoltaic cell via surface plasmon polariton (SPP) modes in an interfacial thin silver contact.

In chapter 2, I discuss the theory underlying how organic PV cells convert light into electricity and describe some of the challenges involved in their design. I describe in detail the nature of the tradeoff between light absorption and charge separation efficiency. In addition, some of the previous methods that have been employed to improve organic PV efficiency, including those aimed at maximizing light absorption near charge separation interfaces, are discussed.

The design and optimization of organic PVs with external antennas are discussed in chapter 3. I discuss energy transfer via guided SPPs and modeling results showing the potential of this architecture. Chapter 4 discusses the experimental fabrication and characterization of organic PV cells with external antennas. The energy transfer efficiency between an external antenna and organic PV cell is calculated. Finally, chapter 5 explores the potential implications of these results and catalogs potential next steps and future directions for external antennas integrated with organic solar cells.

Chapter 2

Organic Photovoltaics

2.1 Mechanism of Power Conversion

Early organic photovoltaic (PV) cells were composed of a single organic semiconductor sandwiched between two metal electrodes with different work functions.[9] The rectification seen in these devices was due to the formation of a Schottky Barrier between the organic layer and the metal contact with the lower work function.[10] While these devices prompted interest in using organic semiconductors in PV cells, their power conversion efficiencies were extremely poor.

The introduction of the bi-layer heterojunction device architecture first demonstrated by Tang in 1986 was a major step forward.[11]. Similar to inorganic semiconductor pn-junction solar cells, organic heterojunction solar cells are constructed from two distinct semiconducting layers placed between metal electrodes. In inorganic devices the p and n layers are created by oppositely doping two adjacent volumes of the same semiconductor. In contrast, organic heterojunction solar cells employ a different semiconducting material for each layer, one having good transport properties for holes (also known as a donor layer) and the other favoring the transport of electrons (also known as an acceptor layer). In inorganic cells the electric field generated by the pn-junction acts to separate excited charge pairs.[12] In organic materials, the energy-level offset of the two different materials is needed due to the more localized nature of excitations. This means that the power generation mechanisms for organic

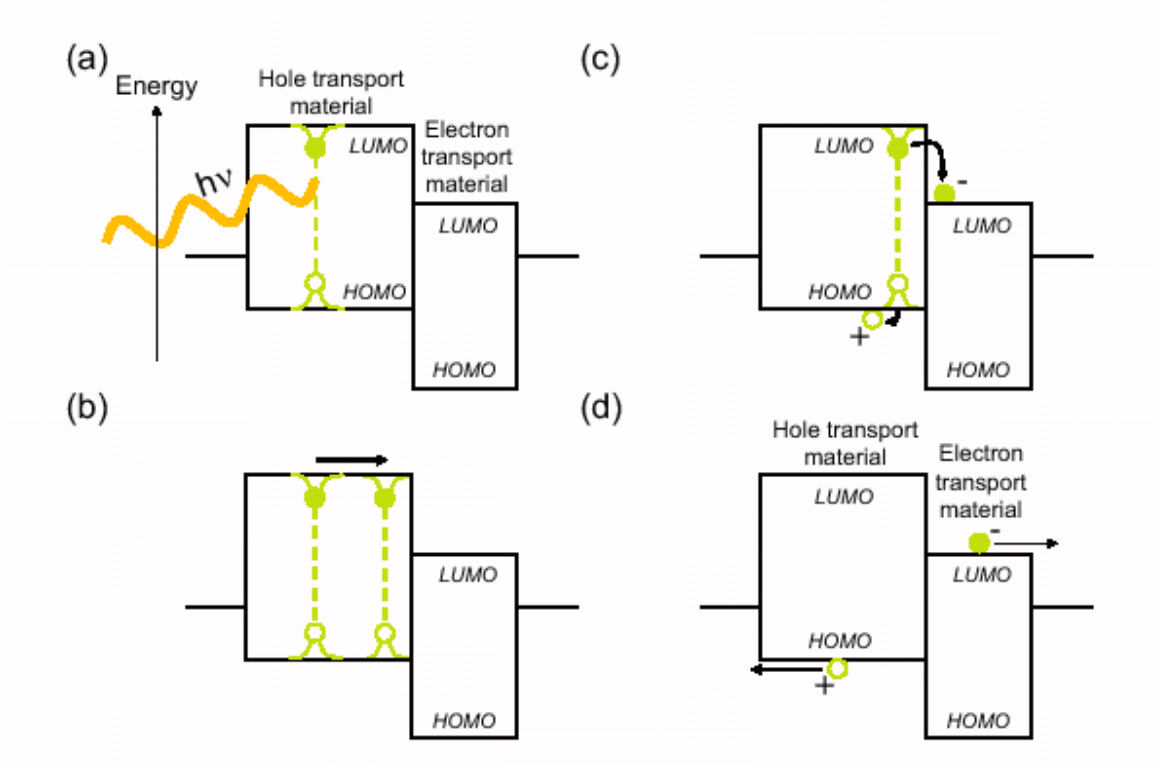

Figure 2-1: **Summary of power conversion processes in organic PV** (a) Optical absorption in one or more of the semiconducting layers creates locally bound electron-hole pairs or excitons. (b) Excitons diffuse in the semiconducting layer. (c) Excitons reaching the interface between the acceptor and donor semiconducting layers before recombination are dissociated. (d) Separated electrons and holes diffuse to opposite electrodes. After Peumans et. al.[13]

cells are fundamentally different than those found in conventional inorganic devices. Given below is a basic overview of the primary power conversion processes found in organic photovoltaics. For a more thorough discussion of these processes I direct the reader to the review by Peumans,2003.[13]

The conversion of light into electrical power can be separated into four distinct steps as illustrated in Fig. 2-1. The absorption of light in one of the semiconducting layers initiates the process. Optical absorption generates tightly bound, charge-neutral hole and electron pairs referred to as Frenkel or charge transfer excitons.[14] The weak intermolecular interactions and lack of long range order found in organic semiconductors gives rise to highly localized excitons. In order to extract power from the device, the excitons must be separated into their constituent charges. This sepa-

ration occurs if the excitons diffuse to the interface between the donor and acceptor layers before they recombine. Organic heterojunction PV cells are designed such that the energy level offsets at the interface between the two semiconductors makes it energetically favorable for the charges to separate. Charge separation results in electrons being found in the lowest unoccupied molecular orbital (LUMO) of the electron transport layer and holes in the highest occupied molecular orbital (HOMO) of the hole transport layer. Finally, the separated charges diffuse toward the contacts generating power.

The external quantum efficiency (η_{EQE}) of the cells, defined as the number of electrons flowing in the external circuit per photon incident on the PV cell, is a function of the efficiency of each of the internal processes described above:

$$\eta_{EQE} = \eta_{abs} \times \eta_{diff} \times \eta_{diss} \times \eta_{cc} \tag{2.1}$$

where η_{abs} is the efficiency of photon absorption leading to creation of an exciton, η_{diff} is the efficiency that an exciton created in the semiconducting layers will reach the donor-acceptor interface, η_{diss} is the efficiency of the dissociation of excitons that reach the interface, and η_{cc} is the efficiency with which separated charges are collected at the electrodes.

The large energy offsets at the donor-acceptor interface result in charge separation occurring over timescales of a few hundred femtoseconds.[15] This leads to efficiencies of charge separation near 100%. In addition, the effiency of charge collection, η_{cc}, is near 100% for these devices. Therefore, the absorption efficiency and exciton diffusion efficiency are left as the major barriers to high power conversion efficiencies. Unfortunately, these two efficiencies are mutually exclusive in conventional device architectures; increasing absorption by increasing the device thickness leads to a decrease in exciton diffusion efficiency and vice versa.

2.2 Light Absorption vs. Charge Separation

The tradeoff between charge separation efficiency and optical absorption drives much of the current research in organic photovoltaics. Exciton diffusion lengths, L_D, for organic materials are typically on the order of 10nm. This is much shorter than typical optical absorption lengths ($(1/\alpha) \approx$ 50-100nm). This means that despite being composed of highly absorptive organic materials with absorption coefficients exceeding 10^{-5} cm^{-1}, organic PV cells are limited by the amount of light they can absorb. Only the light absorbed near the interface between layers contributes to generated power.

2.3 Architectures Employed to Improve Efficiency

Several novel device architectures have emerged that aim to overcome the tradeoff between light absorption and charge separation efficiency including bulk organic heterojunction cells, dye-sensitized nanostructured oxide cells, and tandem or stacked cells.

2.3.1 Bulk Heterojunction Cells

Bulk heterojunction organic photovoltaic cells were first demonstrated using blends of donor and acceptor semiconducting polymers.[16] Upon deposition (usually via spin coating) and subsequent solvent evaporation, the polymers have been shown to phase separate forming an interpenetrating network.[17] This vastly increases the interfacial surface area between the materials, decreasing the average distance between exciton generation and dissociation.

However, this technique is limited by the necessity for continuous pathways within the two phases for charge collection at each electrode. Reduced charge carrier mobilities due to intermixing on the molecular level can lead to recombination of separated charges. Nonetheless, this technique has led to significant improvements in the efficiency of polymer devices with internal quantum efficiencies demonstrated as high as

85% at some wavelengths and power conversion efficiences as high as 3.5% under 1 sun, AM1.5 solar illumination.[18] Efforts at improving polymer bulk heterojunction cells have included optimizing the relative concentraions of each polymer in solution as well as the exploration of postproduction treatments such as annealing.[18]

More recently, the bulk heterojunction concept has also been demonstrated in cells utilizing co-evaporated small molecule organics.[19] However, simply co-depositing the two materials leads to devices with very poor charge collection as the materials do not readily phase separate, as illustrated in Fig 2-2. It was found that increasing the substrate temperature during growth leads to phase separation and crystalline domains. However, increasing the substrate temperature also results in rougher films that suffer from pinholes resulting in short circuited devices. Post deposition processing also leads to poor device yields with many short circuited devices. Using an underlying layer of a mixture of poly(3,4-ethylenedioxythiophene) (PEDOT) and poly(styrenesulfonate) (PSS) was found to help planarize the cells. Cells composed of pentacene and a perylene derivative were also successfully demonstrated with power conversion efficiencies as high as 0.54%.[20]

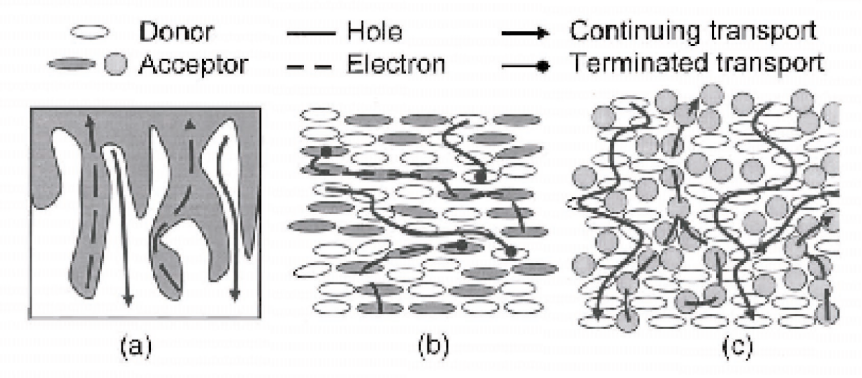

Figure 2-2: **Illustration of conduction in bulk heterojunction mixed semiconductor layers** (a) Idealized interdigitated structure of donor and acceptor layers with lateral feature sizes no larger than the exciton diffusion lengths. (b) Poorly structured mixing of donor and acceptor molecules with few pathways for hole and electron conduction leading to trapping and recombination. (c) Improved mixing conditions with continuous pathways for hole and electron conduction after exciton dissociation. After Xue et al. [21]

An extension of the bulk heterojunction cell architecture for co-evaporated small

molecules has emerged under the names of hybrid planar-mixed heterojunction (PM-HJ) and organic p-i-n solar cells.[22][21][23] Both of these names refer to cells with co-deposited mixed layers of organic semiconducting materials sandwiched between neat films of hole and electron transporting semiconductors. The mixed layer is intended to increase the surface area of the interface allowing more light to be absorbed while the neat films assist in charge collection and eliminate problems with short circuit devices.

2.3.2 Dye-Sensitized Nanostructured Oxide Cells

Another strategy utilized to increase the light absorption efficiency of organic solar cells while not reducing charge separation efficiency has been the design of dye-sensitized nanostructured oxide cells. These cells accomplish optical absorption and charge separation using two separate materials: a wide-bandgap semiconductor of mesoporous or nanocrystalline morphology such as TiO_2 is coated with a monolayer of dye.[24] The dye-coated inorganic oxide electron conductor is combined with either an electrolyte solution or a solid-state molecular hole-conducting material. Upon absorption of light in the sensitizer dye, an electron is injected into the conduction band of the semiconducting oxide. The electron is then transported to the anode where it can be collected and perform work in an external circuit. The hole conducting material serves to regenerate the sensitizer and transport positive charges to the counter electrode. The use of sensitizers with broad absorption bands has the potential to allow cells to harvest a large fraction of the solar spectrum.

Cells utilizing electrolyte solutions have achieved efficiencies as high as 11% while solid state cells using molecular hole conductors have been demonstrated with a maximum efficiency of 4%.[25] Solid-state nanostructured oxide cells have the benefit of not requiring the encapsulation of liquid electrolyte solutions. Quasi-solid-state devices utilizing polymer electrolyte gels have also been demonstrated.[26] An example of this architecture is given in Fig. 2-3. Recent work has expanded the range of nanostructured materials used in dye-sensitized cells. Devices with dense arrays of oriented, crystalline ZnO nanowires and CdSe nanorods have been demonstrated.[27][28]

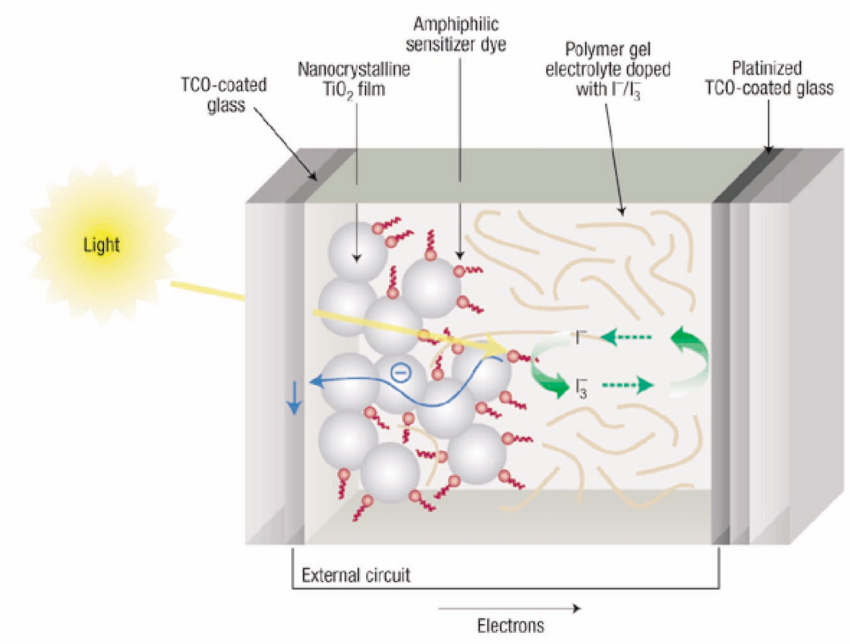

Figure 2-3: **Schematic illustration of the dye-sensitized nanostructured oxide cell architecture.** A mesoporous, nanocrystalline TiO_2 film (the grey spheres) sensitized by a dye (the red molecules) with polymer gel electrolyte (brown lines) interpenetrated into the film pores. The device is sandwiched between two transparent conducting oxide (TCO) electrodes. The polymer gel illustrated here has alternatively been substituted by electrolyte solutions and solid state polymer layers. After Durrant and Haque.[26]

2.3.3 Tandem (Stacked) Cells

Devices with multiple, stacked heterojunctions have also been demonstrated.[29] Thin semi-transparent heterojunctions were constructed in layers separated by extremely thin, discontinuous layers of silver clusters. The Ag clusters serve as charge recombination sites for unpaired charges generated in the interior of the device. In the design of these so-called "tandem cells," the optical absorption of each individual heterojunction must be balanced so that the photocurrent from each heterojunction is approximately equal. In principle, each heterojunction can be designed to absorb a separate part of the solar spectrum. This is especially attractive as most materials only absorb strongly over a narrow range of wavelengths. In addition, stacking the cells has the effect of significantly increasing the open circuit voltage for the devices. The total open circuit voltage is simply the sum of the built-in voltages of each

individual cell.

Initial demonstrations of tandem cells resulted in power conversion efficiencies nearly double those using single heterojunctions with the same materials.[29] Subsequent efforts stacking hybrid planar-mixed heterojunctions have resulted in the demonstration of cells with power conversion efficiencies as high as 5.7%.[8] The fabrication of polymer-based tandem cells is complicated by the need to spin coat multiple layers; the lower layers in the cells can be destroyed by the solvent used in susequent layer depositions. Nonetheless, working polymer stacked structure devices have recently been demonstrated with power conversion efficiencies as high as 2.6%.[30]

2.4 Light Trapping Strategies

While the above efforts focused on expanding the surface area of the charge separation interface in devices, additional efforts have focused on trapping light in PV devices more effectively. This has been accomplished by modeling optical field intensities within devices,[31][32] by using diffraction gratings,[33][34][35] and by utilizing the field enhancing properties of metal nanoclusters.[36][37]

2.4.1 Optical Modeling

Modeling the optical interference in devices has proved to be a technique that can be used to increase the light absorbed in organic PV structures while making only minor changes to layer thicknesses.[31] The generation of excitons at a given position in a device is dependent on the optical electric field intensity at that position. Reflections at each interface in the device modify the electric field distribution. Using matrix methods and the optical constants of each material, the reflection and transmission coefficients can be determined numerically. These values can then be used to determine the location of optical electric field intensities. To maximise device efficiency, the maxima in the field intensities should be centered on the charge separation interface.

Figure 2-4, from Pettersson et al.,[38] illustrates this method of optimizing layer

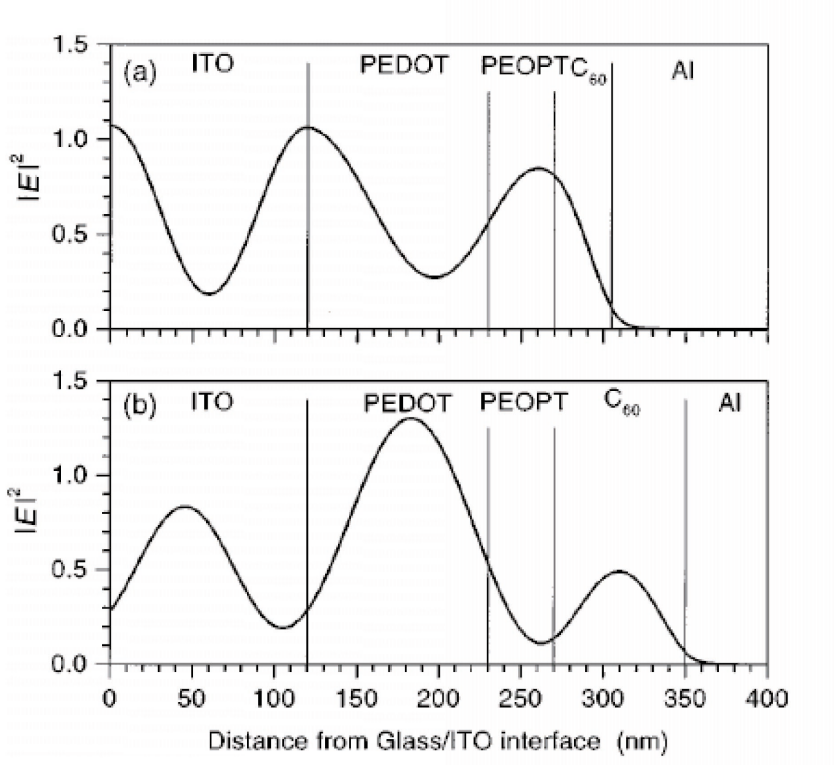

Figure 2-4: **Optical field modeling in organic PV** (a) The layer thicknesses in this device result in an optical field maximum being located at the interface between the active PEOPT and C_{60} semiconducting layers. Locating the interference maximum at this point improves the efficiency of the device. (b) Devices with a slightly thicker C_{60} layer have a minimum in the optical field located at the charge separation interface. After, Pettersson et al. [38]

thicknesses. The PV devices illustrated are composed of the same materials but in the top structure the electric field intensity is at a maximum at the charge separation interface between PEOPT and C_{60} whereas in the bottom structure there is minimal field intensity, and therefore minimal absorption, in the vicinity of the interface.

Furthermore, optical interference modeling has been used to predict the wavelength resolved photocurrent or action spectra from devices.[32] Comparisons of the predicted and experimental photocurrents have been used to estimate the diffusion coefficients of various materials.[38]

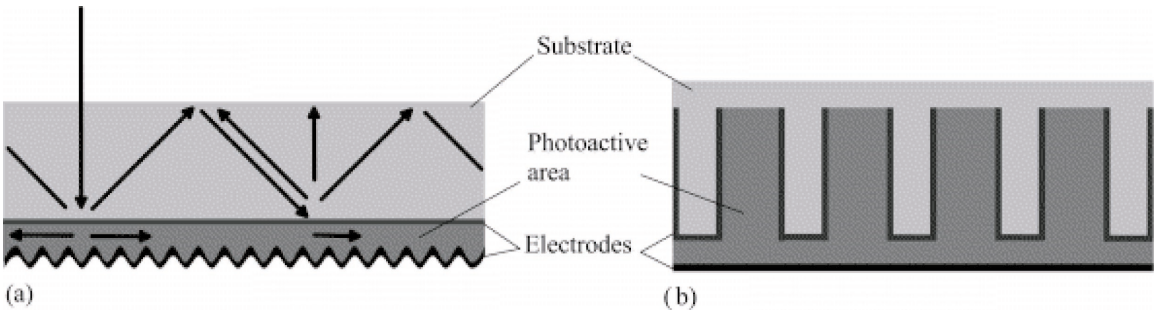

Figure 2-5: **Schematic drawings of two light trapping architectures** (a) Patterning the electrode to form a diffraction grating is one method that has been employed to trap incident light in organic PV structures. The arrows represent theoretical pathways taken by the incident light in this structure. (b) Buried nano-electrodes have also been used to increase the interaction distance between light and the organic PV active semiconductors. After Niggemann et al. [34]

2.4.2 Diffraction Gratings and Buried Nanoelectrodes

The use of diffractive optical structures built into devices has also been explored as a means of increasing light absorption. Several different implementations have been demonstrated. In one, a soft embossed grating was built into an active layer polymer.[33] The structure was designed to diffract incident light into guided modes in the thin polymer film. In other attempts, a comb-like array of electrodes embedded in a polymer were used. As shown in Fig. 2-5 the structure of the electrodes was designed to diffract the incoming light producing an absorption maximum in the active layer.[34]

A similar effort was made building solar cell devices on top of a structured substrate.[35] The substrate was structured to act as a prism reflecting the light through the active layers of the solar cell multiple times. Significant optical modeling is still needed to design optimized diffraction gratings and/or substrate shapes. This approach shows great potential as a way to separate the optical and electrical components of solar cells. The design of the diffraction gratings and substrate shapes is essentially independent of the layer thicknesses used in the actual conversion of light energy to electrical power. The solar cell can be designed first, and a diffraction grating optimized for that cell could be designed subsequently. However, structures can typically only be optimized for a single wavelength of incident light.

2.4.3 Metal Nanoclusters

Incorporating metal nanoclusters in devices has also been used as a method to increase efficiency in organic photovoltaic cells. Several theories have been advanced as to the nature of the increase in photocurrent observed when metal nanoparticles are added to a semiconducting layer. One theory proposes that the electric field is strengthened in the vicinity of metal nanoclusters incorporated into thin films of semiconducting materials. This strengthening of the electric field increases absorption in the surrounding organic material leading to a greater photocurrent.[39] Another theory posited that exciton plasmon modes in the metal clusters themselves could emit an electron leading to an increased current.[40] Plasmon excitations are discussed more in the following chapter as they are the means of energy transfer relevant to this thesis.

Metal nanoclusters have been incorporated in many of the device architectures discussed above including dye-sensitized cells[36] and tandem cells where silver nanoclusters were used between heterojunctions.[37] In this final implementation the optical field close to the nanoclusters was found to have increased by up to a factor of 100 compared with the incident light intensity.

Chapter 3

A Device Architecture Inspired by Photosynthesis

The widespread harvesting of energy from the sun has, as yet, been beyond the reach of humans. In contrast, plants, algae, and bacteria have mastered the process over millions of years of evolution. Photosynthesis, the biochemical process that nature uses to convert sunlight into chemical energy provides the great majority of the energy used on Earth. Therefore, it seems only natural that photosynthesis might be an ideal place to look for inspiration in building electronic devices to harvest the sun's energy.

In photosynthesis, light absorption and exciton dissociation occur in spatially separated components: light absorption occurs in an antenna complex while exciton dissociation occurs in a complex known as a reaction center.[41] In contrast, in the architectures for organic PV, absorption, exciton dissociation and charge extraction all occur in the organic semiconductors comprising the donor and acceptor layers. Therefore, the semiconductors chosen for use in organic PVs must satisfy several constraints including: (1) strong, broadband optical absorption that overlaps well with the solar spectrum, (2) efficient long range exciton transport, (3) energy level offsets allowing for efficient exciton dissociation, and (4) high electron and hole mobilities with continuous charge conduction pathways between the two electrodes.[42] It is very difficult to find materials satisfying these multifarious requirements.

As in photosynthesis, the spatial separation of optical absorption and exciton

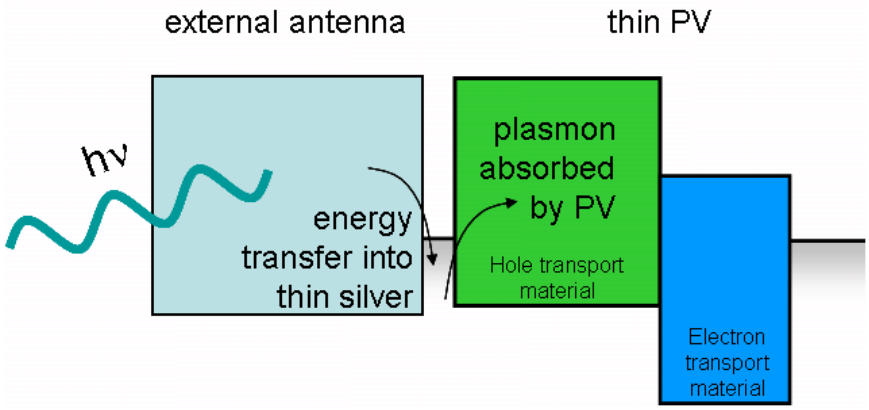

Figure 3-1: **Organic PV with an external antenna** In the device architecture proposed here, an external antenna layer is added adjacent to one of the electrodes. Light is absorbed in the antenna layer and transferred to the PV via surface plasmon polariton modes in the thin silver electrode. Energy transfer to the PV results in the generation of excitons which follow the same energy transduction pathways as in an organic PV without an antenna.

dissociation in organic PV would allow the independent optimization of each, eliminating the tradeoff discussed in chapter 2. Here, we mimic the architecture found in photosynthesis in organic PV by spatially separating optical and electrical functions. As illustrated in Fig. 3-1, in our device, energy transduction begins with photon absorption in an artificial antenna. Excited molecular dipoles in the antenna are coupled to a thin charge generation cell akin to a traditional organic bilayer heterojunction. Energy transfer is mediated via surface plasmon polaritons (SPP) and radiation into waveguide modes. Using an external antenna for light absorption allows for the design of very thin organic PV charge separation 'reaction centers' with internal quantum efficiencies approaching 100%.

3.1 Energy Transfer via Surface Plasmon Polariton Modes

In the device structure proposed here, excited molecular dipoles in the antenna transfer energy to the PV cell via surface plasmon polariton (SPP) modes associated with the adjacent silver electrode. SPPs are guided electromagnetic waves comprising a

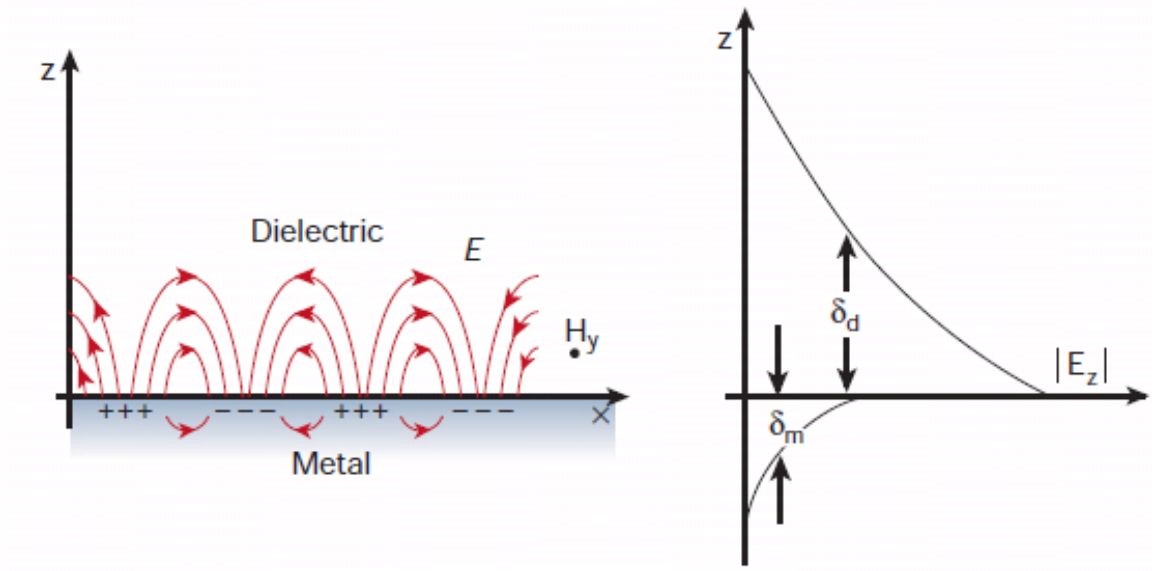

Figure 3-2: **Surface plasmon polariton orientation and field enhancement** Surface plasmon polaritons are transverse magnetic with electric field components both normal to the surface and in the propagation direction. Significant field enhancement exists at the interface and decays exponentially into each adjacent medium.

coupled oscillation of an electromagnetic field and surface charges at metal-dielectric interfaces.[43] Interest in SPPs has grown significantly in recent years as nanometer scale control over metal surfaces and structures has become possible.[44][45] Applications of SPPs span many fields including optics, microscopy, and sensors.[46][47][48]

As illustrated in Fig. 3-2, SPPs propagate along interfaces between metals and dielectrics and are highly localized within the interface area.[43] The modes are tranverse magnetic with electric field components both normal to the surface (due to the existence of surface charge) as well as in the propagation direction. The enhanced field is evanescent, decaying exponentially into both adjacent media. The characteristics of SPPs are strongly dependent on both the refractive index of the dielectric material as well as the complex dielectric function and surface roughness of the metal. SPPs can be excited at interfaces between metals with negative dielectric functions and dielectric media with positive dielectric functions. Excitation of SPPs results in an enormous field enhancement at the propagation interface.

Enhancement of organic solar cell efficiency by excitation of SPPs has been demonstrated previously.[49][50] However, photons cannot directly couple with SPPs, so

previous attempts have employed the attenuated total reflection (ATR) method to excite SPPs.[42]

As illustrated in Fig. 3-3, photons cannot directly couple with SPPs since their dispersion curves never cross. SPPs have extra momentum associated with the oscillating charges which shifts their dispersion curve to the right of the photon's dispersion line.[43] The requirement that energy and in-plane momentum always be conserved, therefore, prevents the two modes from coupling directly. The ATR method overcomes this limitation by inserting a second dielectric material with a dielectric constant larger than the original dielectric above the interface.[51][52] This is often accomplished by using a high index glass prism that shifts the dispersion line for light incident on the metal surface to the right. Adjusting the angle of incidence allows one to access all momentums to the left of the new dispersion curve. Changing the angle of incidence selects a specific in-plane momentum. Therefore, for a given energy photon (wavelength of light) one can couple to plasmons by choosing an appropriate angle of incidence. The excitation of SPPs using the ATR method was shown to have increased the short circuit current in organic solar cells by a factor of almost 8 at a specific wavelength.[49]

The angular dependent nature of the ATR method and need for an external prism limit the practically of such an approach for solar cells. An alternative approach, employed here, is to use excited molecular dipoles to couple to SPPs. Dipole coupling to SPP modes in a multilayer stack has been explored both theoretically [53][54] and experimentally.[55] To examine energy transfer within a multilayer organic PV stack, we adapt the method of Chance et al.[53] and model antenna excitons as oscillating charge dipoles. The near-field of a dipole contains components of a large range of wavevectors and therefore, can be considered to have a horizontal dispersion line. The horizontal dispersion curve intersects the SPP dispersion curve, thus allowing coupling.

Several decay channels are available for the oscillating electric field associated with a radiative dipole at an excited molecule in the antenna. The field can decay non-radiatively into phonons. The field can radiate photons into free space modes.

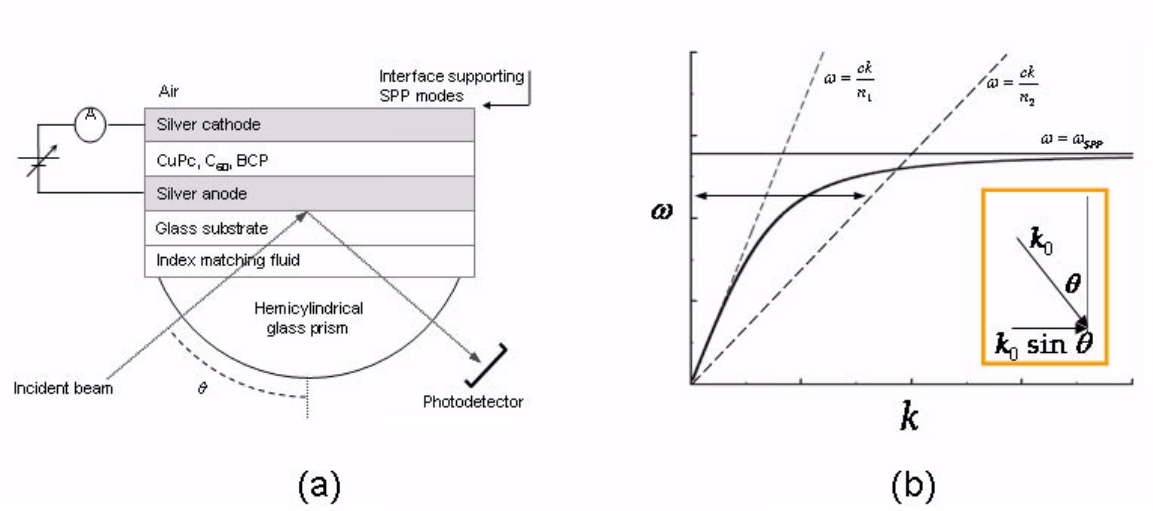

Figure 3-3: **Attenuated total reflection test setup and surface plasmon polariton dispersion relation** (a) In the attenuated total reflection measurement setup an external prism is used with varying angles of incident light to excite plasmons directly from light. (b) Incident photons have straight line dispersion curves. The surface plasmon polariton (SPP) is represented by the solid curved line. The light line on the left never crosses the SPP dispersion curve. Therefore, light incident in the medium with index of refraction n_1 cannot couple with the surface plasmon. In contrast, light incident in the medium with index of refraction n_2 can couple with SPPs at one specific angle.[42]

The radiation can also be channeled into dielectric waveguide modes in the multilayer stack. Finally, the energy associated with the field can be non-radiatively transferred into surface plasmon polariton modes at the adjacent metal interface.

For efficient dye molecules in isolation, radiation into photon modes is the dominant process. However, in the vicinity of a multilayer stack composed of both metal and dielectric layers, emission into both waveguide modes and surface plasmon modes can dominate. The rate of free space emission is dependent on the photonic mode density by Fermi's golden rule. Near a metal film, the photonic mode density drops dramatically as visible light is strongly absorbed by the free charges of the metal.[56] Therefore, non-radiative energy transfer to guided electromagnetic modes is favored.

Energy transfer has been demonstrated from excited molecules to SPP modes in metallic slabs [57][56] and thin films[58] at nearly unity efficiency.

3.2 Simulation of Energy Transfer Efficiency

We performed simulations of the energy transfer efficiency from an antenna to a bilayer organic heterojunction PV structure utilizing common organic electronic materials. The initial structure used in the modeling was composed of a silver anode (Ag, 400Å) underlying layers of copper phthalocyanine (CuPc, 270Å), 3,4,9,10-perylenetetracarboxylicbis-benzimidazole (PTCBI, 270Å), bathocuproine (BCP, 100Å), and silver (Ag, 130Å). Aluminum tris(8-hydroxyquinoline) (Alq_3), a material studied extensively in organic light emitting diodes, was chosen as an antenna material to use in simulations. The structure was modeled on a glass substrate. The indices of refraction and extinction coefficients of all modeled thin films were directly measured using an Aquila nkd8000 spectrophotometer. Software associated with the spectrophotometer allows the user to determine the optical constants from reflection and transmission data taken with multiple polarizations of incident light.

Results of device simulations are illustrated in Fig. 3-4. The energy coupling is dependent on the transition dipole orientation with respect to the plane of the interface. Therefore, perpendicular (Fig. 3-4a) and parallel (Fig. 3-4b) orientations

are considered separately.

The coupling fraction of antenna excitons as a function of distance from the Alq_3-Ag interface and normalized propagation constant, u, are shown in Fig. 3-4a and Fig. 3-4b. The normalized propagation constant, u, is defined as the wavevector normalized by the wavevector of an unconfined photon in the far field. Values of $u < 1$ correspond to radiative modes (including photon emission and waveguide modes) while values of $u > 1$ correspond to non-radiative energy transfer.

Coupling to SPPs is strongest close to the thin silver contact. For dipoles oriented parallel to the interface, both dielectric waveguide and SPP modes are significant. Dielectric waveguides dominate at distances farther from the thin silver where coupling to SPPs is unlikely.

Two prominent SPP modes can be found in the simulated plots of coupling fraction. The broad peak at normalized propagation constant $u = 1.8$ corresponds to an enhanced field localized at the antenna-silver interface. The field intensity profile for this propagation constant value is shown in Fig. 3-4c. As shown in Fig. 3-4d, the other, narrow peak in the coupling fraction with propagation constant $u = 1.1$ corresponds to an enhancement at the glass-silver interface.

The efficiency of energy transfer from the antenna to the semiconductor layers making up the charge generation cell was calculated by extending the method of Chance et al. [53] to evaluate the Poynting vector, $\vec{P}$.[59]

In an isotropic film, the transition dipoles will be 1/3 perpendicular and 2/3 parallel. Therefore, in estimating overall energy transfer, the coupling fractions for perpendicular and parallel dipoles have been weighted appropriately. The overall energy transfer, shown in Fig. 3-5, was estimated by calculating $\vec{P}$ within the active semiconductor layers of the charge separating structure for each u and integrating over all u. In anticipation of using DCM as a dopant in experimental devices, we assumed that the Alq_3 antenna was doped with a randomly-oriented fluorescent dye with a photoluminescent (PL) efficiency of 70% and an emission wavelength of $\lambda = 615$ nm. In the unoptimized PV illustrated in Fig. 3-5, the average efficiency of energy transfer to the PV layers is 52% over the thickness of the antenna layer.

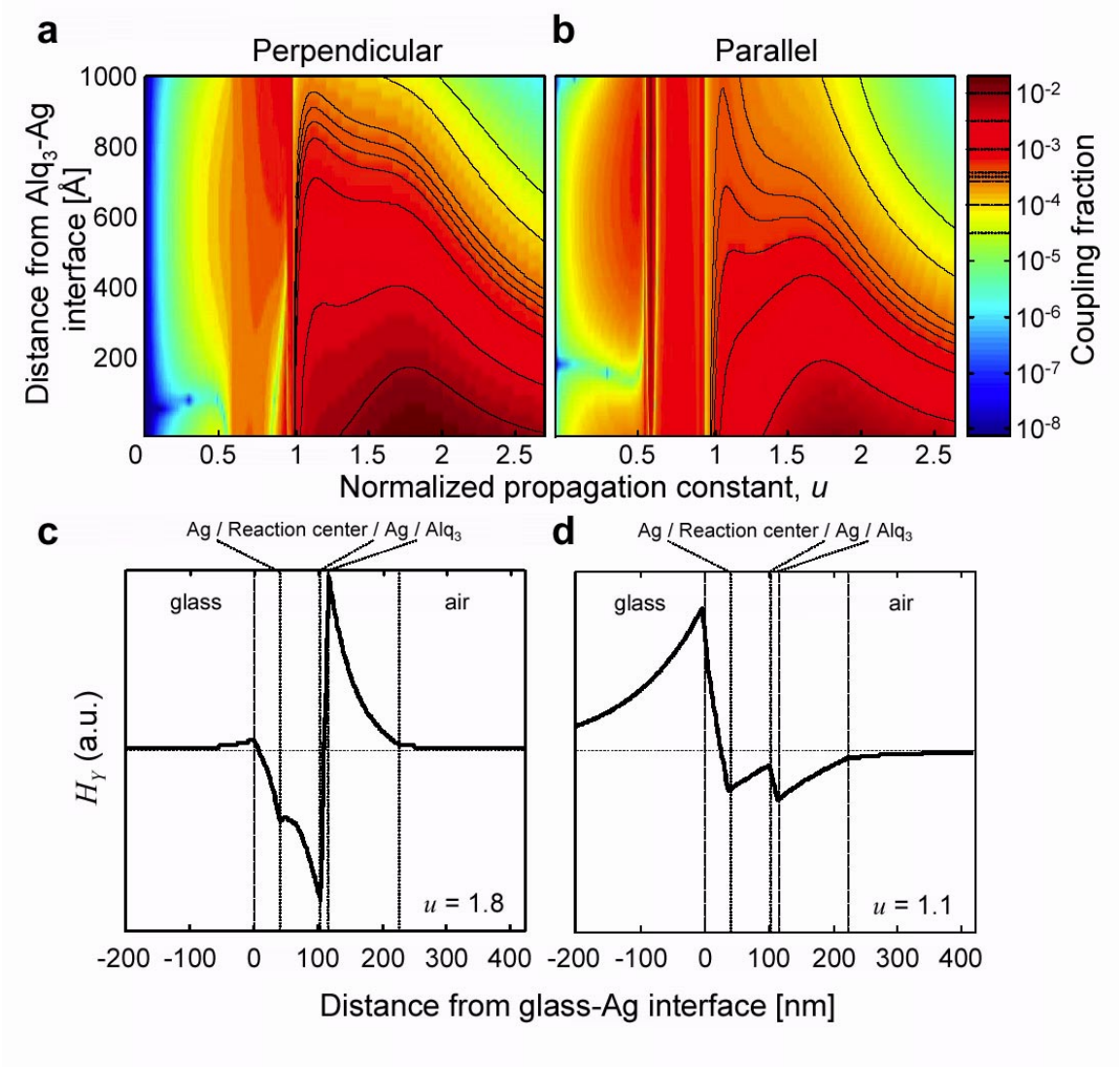

Figure 3-4: **Exciton coupling fraction and mode profiles** Logarithmic plot of coupling as a function of distance from the antenna/silver interface and the propagation constant, u. Contours have been added (for u > 1 only, dotted lines on colorbar) to emphasize peaks in coupling fraction. (a) Coupling into non-radiative modes with u > 1 is strongest for perpendicularly oriented dipoles. (b) Coupling to dielectric waveguide modes with u < 1 is strongest for dipoles oriented parallel to the Ag-antenna interface. (c) The dominant SPP mode at u = 1.8 is localized at the antenna/cathode interface and has significant overlap with the active semiconducting layers. (d) The u = 1.1 mode is localized at the glass/anode interface resulting in much weaker coupling. The mode profiles were calculated by artificially setting absorption losses to zero in each layer, and calculating the stationary states of the stack.

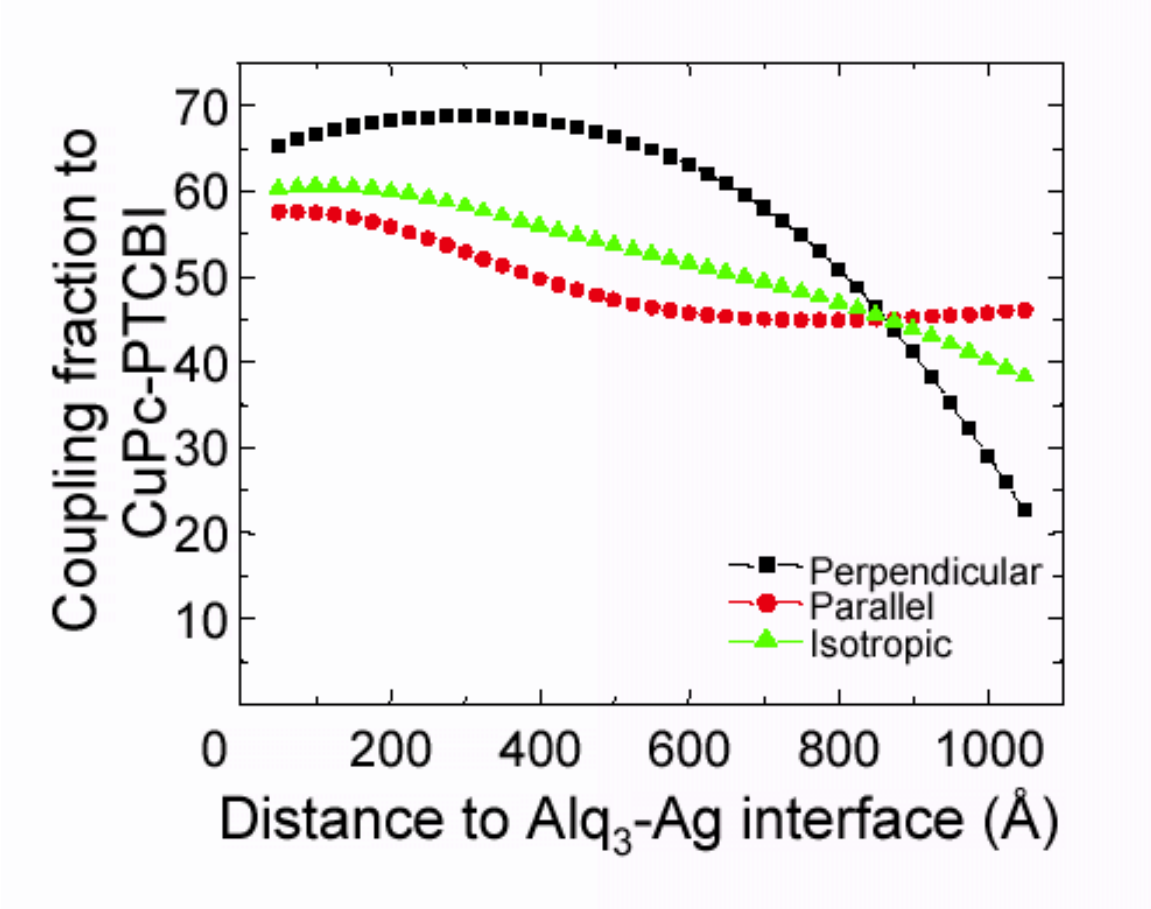

Figure 3-5: **Antenna energy transfer efficiency to organic layers** Efficiency of energy transfer from the antenna to the charge separating cell is highest close to the Alq_3-Ag interface. Over the first 1000Å, the mean exciton coupling fraction to the organic layers is 52% for an isotropic distribution of dipoles.

3.3 Device Design Optimization

Many different structures were simulated in order to find an optimal design. The most important aspect of designing optimal PVs with external antennas was found to be the thickness of the silver cathode separating the antenna layer and PV semiconductor layers. The SPP mode field enhancement extends into both adjacent media when the silver is thin. When the silver layer is thicker, the SPP mode is confined on one side where it cannot mediate energy transfer. We found an optimal silver thickness to be approximately 120Å. Unfortunately, it was not possible to fabricate devices with continuous silver films only 120Åthick on top of the other organic PV layers. Therefore, in the devices discussed in Chapter 4, thicker silver films are used.

The PL efficiency of the antenna was also found to be very important in how efficient energy could be transferred to the internal semiconducting layers. The PL spectrum of the antenna also must overlap well with the internal semiconducting layers. An optimal PV device for use with an antenna layer would be optimized for absorption and charge separation at the energy of the PL emission in the antenna layer.

Chapter 4

Demonstration of Organic PV with External Antennas

Devices were fabricated with several different materials serving as an external antenna. Characterization of the devices involved determining the current-voltage characteristics in darkness and under simulated solar radiation, measuring the wavelength resolved photocurrent action spectra, and measuring the relative PL efficiency of different antennas. Ultimately, the results were used to estimate the efficiency with which energy was transferred from the antenna to the charge generating cell.

4.1 Fabrication of Organic PV

Organic PV devices with integrated external antennas were fabricated by thermal evaporation of all layers onto glass slides. The thermal evaporator was housed within an oxygen and moisture free, nitrogen filled glove box. All processing occurred within the glove box and devices were not exposed to atmosphere until just before measurement. Prior to use, glass slides were cleaned by sonication in detergent (5 minutes), water (10 minutes), and acetone (4 minutes) sequentially. The slides were immersed in boiling isoproponal (4 minutes) and finally placed in a UV/Ozone cleaner (5 minutes).

Where specified below, a mixture of PEDOT/PSS was spun (40 sec, 3000rpm,

1000rpm/s ramp) onto the clean glass slides to improve device yield by planarizing the bottom surface. Substrates with PEDOT/PSS were heated on a hot plate for at least 1 hour prior to use in order to ensure removal of all solvent. Some device structures did not require the use of PEDOT/PSS for acceptable device yields.

Organic materials were purified by vacuum thermal gradient sublimation prior to use. All materials were deposited by thermal evaporation at $\approx 10^6$ Torr. Contacts were patterned by evaporating metal layers through shadow masks. All active device areas were 0.01 cm^2. Thicknesses were measured by profilometry and verified using a spectrophotometer.

Two different antenna materials were utilized, one with high PL efficiency and one with very strong absorption. The search for a material satisfying both of these requirements is ongoing. We chose as our control devices PVs with non-functioning antennas. This avoided changes in the photocurrent spectrum due to interference effects in different device structures. As discussed in section 2.4.1, optical interference effects become important in thin organic PV structures. The efficiency of SPP coupling is proportional to PL efficiency. Therefore, to demonstrate energy transfer via SPP coupling, antennas with varying PL efficiency were fabricated on identical PV charge generation cells.

The first material chosen as an antenna was aluminum tris(8-hydroxyquinoline) (Alq_3). Alq_3 has rarely been employed in organic PVs previously. The structure fabricated was glass/ Ag(400Å)/ CuPc(180 $\dot{A}$)/ CuPc:PTCBI(1:1, 180Å)/ PTCBI(180Å)/ BCP(100Å)/ Ag(130Å)/ Alq3(1070Å). The antenna layer comprised an isotropic mixture of Alq_3 and either the quenching material CuPc or the laser dye 4-dicyanomethylene-2-methyl-6-(p-dimethylaminostyryl)-4H-pyran (DCM) co-deposited at a ratio of 100:1. Comparing the performance of these devices allowed the classification of photocurrent contributions in a functioning antenna PV as originating from either absorption in the antenna or the charge separating active layers.

The second material employed as an antenna was the strongly absorbing dye meso-Tetra(pentafluorophenyl) porphine ($F_{20}TPP$). The structure fabricated was glass/ PEDOT:PSS / Ag (186Å)/ CuPc (245Å)/ Buckminsterfullerene (C_{60}) (195Å)/ BCP

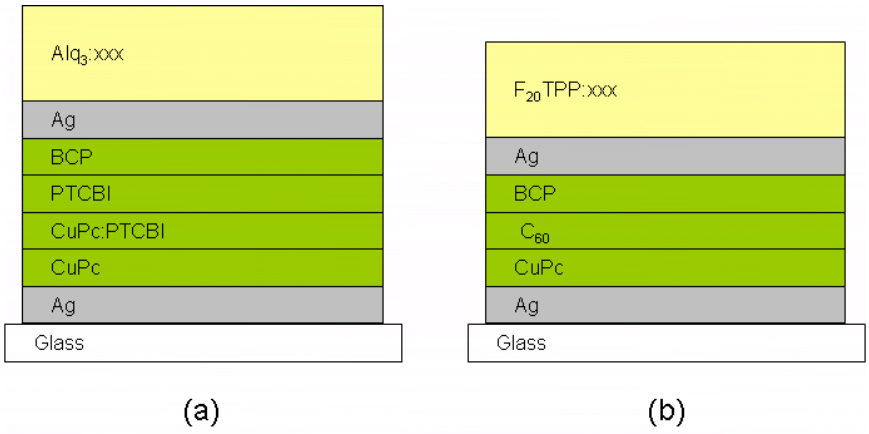

Figure 4-1: **Structures of organic PV devices fabricated with antennas** (a) Alq_3 antennas doped with either CuPc (1%) or DCM (1%) were fabricated on PVs with CuPc and PTCBI acting as active semiconducting layers. A layer of CuPc:PTCBI co-deposited in equal weight ratios was also integrated into these devices. (b) F_{20}TPP antennas doped with either CuPc (4%) or CBP (20%) were fabricated on PVs utilizing CuPc and C_{60} as active semiconductors.

(85Å)/ Ag (150Å)/ F_{20}TPP (700Å). CuPc was once again used as a dopant to quench the PL in the antenna to create non-functional antennas to use as a control. F_{20}TPP was co-deposited with CuPc at a ratio of 25:1. Co-depositing F_{20}TPP and 4,4'-Bis(N-carbazolyl)-1,1'-biphenyl (CBP) was found to increase the photoluminescence efficiency of the antenna. The CBP acts to minimize self-quenching of the F_{20}TPP. F_{20}TPP and CBP were co-deposited at a ratio of 4:1.

4.2 Antenna Photoluminescence Efficiency

The relative PL efficiency of different antennas was determined by fabricating antennas directly on glass with no underlying layers. The antennas were excited with laser irradiation at $\lambda = 408$nm with intensity 0.5 mW/cm^2. PL spectrums were measured using a spectrometer. Fig. 4-2 shows the relative PL spectrums of a neat F_{20}TPP antenna as well as antennas with CBP and CuPc doping. Doping the antenna with CuPc is seen to effectively quench PL while CBP enhances the signal by reducing self quenching of the F_{20}TPP.

Integrating the PL intensity spectrums and normalizing by absorption at the pump

wavelength gives the relative photoluminescence efficiency of each antenna. The doping ratios used were sufficiently low to result in no change in antenna absorption at the laser pump radiation wavelength.

The PL efficiencies of the co-deposited films of Alq_3 with CuPc and DCM relative to neat films of Alq3[60] were measured to be 0% and 75%, respectively. The PL efficiencies of the co-deposited films with CuPc and CBP relative to neat films of F_{20}TPP were measured to be 0% and 4%, respectively.

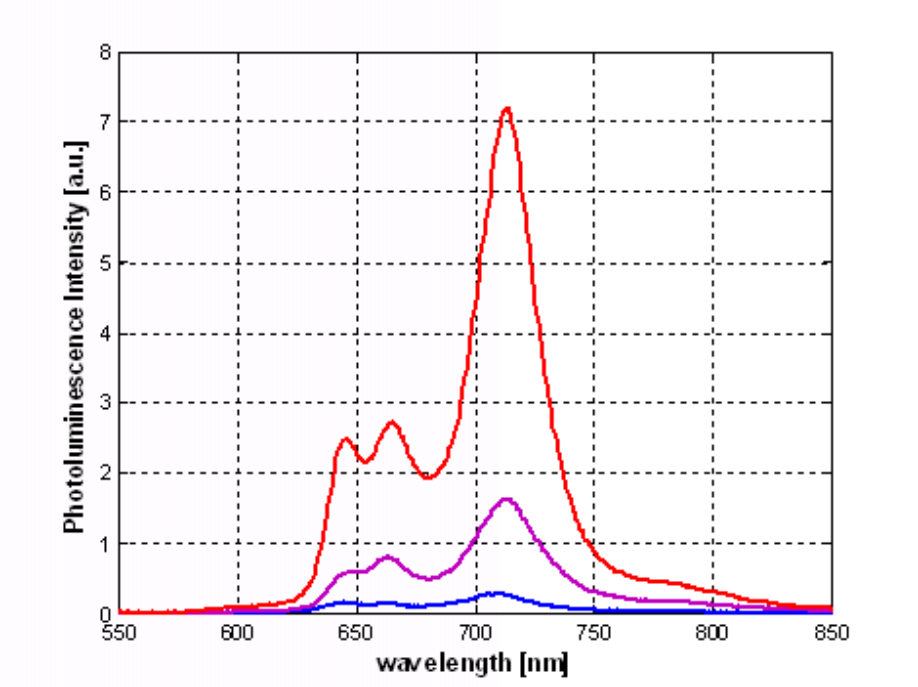

Figure 4-2: **Relative photoluminescence intensity** Peaks in emission from F_{20}TPP are found at 646nm, 665nm and 713nm. Integrating the PL intensities of each antenna and normalizing by absorption gives the relative PL efficiency of the different antenna layers.

4.3 Current-Voltage Characteristics

Illuminated current-voltage measurements were taken with a 1 kW solar simulator (Oriel) filtered to approximately one sun intensity and AM1.5G spectrum and measured with a (HP4156) semiconductor parameter analyzer.

Devices utilizing CuPc and PTCBI as semiconducting layers exhibited typical

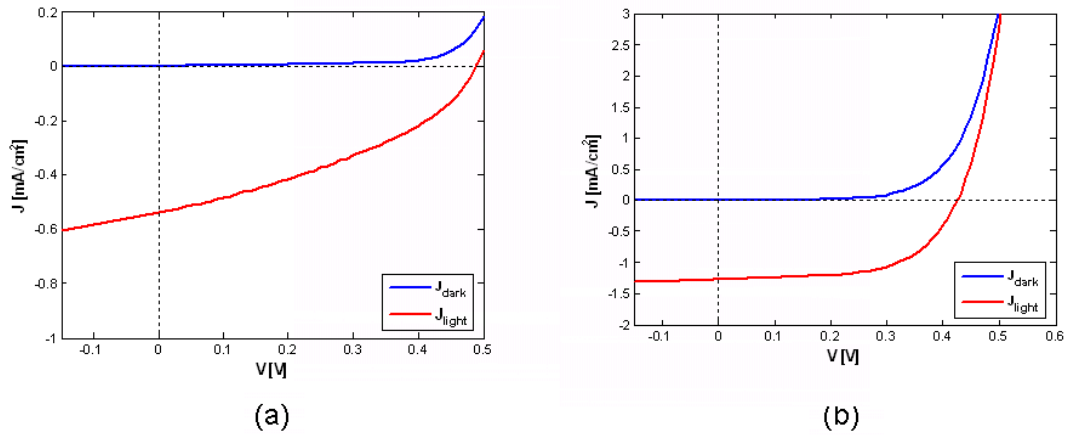

Figure 4-3: **Current-voltage Characteristics** (a) Devices utilizing CuPc and PTCBI as semiconducting layers exhibited typical open-circuit voltages of 0.49V, short-circuit currents on the order of 1 mA/cm^2, and fill-factors of 0.41. (b) CuPc/C_{60} devices were better performing solar cells. The devices exhibited open-circuit voltages of 0.51V, short-circuit currents approximately 1.5mAQ/cm^2, and fill-factors of 0.62. [Note: Different data ranges were chosen when measuring these devices. The scales on the above plots are not the same.]

open-circuit voltages of 0.49V, short-circuit currents on the order of 1 mA/cm^2, and fill-factors of 0.41. CuPc/C_{60} devices were better performing solar cells. The devices exhibited open-circuit voltages of 0.51V, short-circuit currents of approximately 1.5mA/cm^2, and fill-factors of 0.62.

The antenna materials utilized to demonstrate the concept of energy transfer were not strong enough to produce a measurable difference in the current-voltage characteristics. Overall, power conversion efficiencies were the same (within noise limits) for devices with and without functioning antennas.

4.4 Wavelength Resolved External Quantum Efficiency Detection

Photocurrent measurements were made by using a xenon lamp with monochromator, chopped at 90 Hz, and measured using a lock-in amplifier. Incident light intensity was measured with a calibrated silicon photodiode.

External quantum efficiency (η_{EQE}) was calculated using the detected photocurrent as:

$$\eta_{EQE}\% = 100 \times 1240 \times \frac{R}{\lambda} \times \frac{I}{I_r}$$

where R is the responsivity of the calibrated photodiode, λ is the wavelength of incident light, I_r is the photocurrent obtained using the calibrated photodiode, and I is the photocurrent obtained from the PV device.

The correct choice of the control devices became important in taking photocurrent measurements. Devices with and without antennas often had mismatching photocurrent spectrums due to micro-cavity optical interference effects, rather than energy transfer from the antenna.

As shown in Fig. 4-4a, in devices utilizing Alq_3 antennas, the magnitudes of the photocurrents are nearly identical in regions where Alq_3 is transparent. The guest species CuPc and DCM were doped into the antennas at too low a concentration to make any measureable difference in the antenna absorption spectrum. In the region of $350 < \lambda < 450$ nm, where Alq_3 absorption is the strongest, the devices with functioning antenna layers exhibit increased quantum efficiency. A 30% peak increase in photocurrent was found for devices with Alq_3:DCM(1%) antennas relative to devices with non-functioning Alq_3:CuPc(1%) antennas.

In addition, as illustrated in Fig. 4-4b, the shape of the increase in photocurrent matched well with the shape of Alq_3 absorption. The peak of the relative photocurrent increase was found slightly red-shifted from the absorption peak of neat films of Alq_3 measured with no underlying layers. The overall gain in η_{EQE} is limited by low absorption in the antenna layer and relatively small η_{IQE} in the unoptimized PV cell.

An increase in η_{EQE} matching the antenna absorption spectrum was also found when using F_{20}TPP antennas. F_{20}TPP is an attractive material for use as an antenna due to its very strong absorption. The strongly absorbing Soret band of the material was found to absorb more than 70% of the incident light at wavelengths shorter than 450nm in films 750Åthick. The devices in Fig. 4-5 had matching antenna absorption

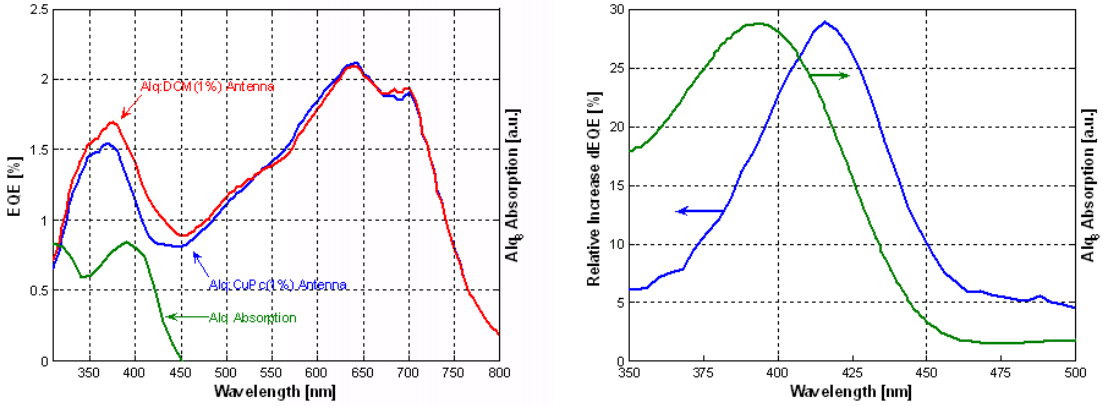

Figure 4-4: **Alq_3 antenna external quantum efficiency enhancement** (a) The external quantum efficiency is higher for devices with a functioning Alq_3:DCM(1%) antenna relative to those with non-functioning (quenched) Alq_3:CuPc(1%) devices. Alq_3's absorption is strongest near 400nm. (b) The peak increase in EQE in devices with functioning antennas is 30% relative to those with non-functioning antennas. The increase in EQE has the same shape but is red-shifted slightly from the absorption of Alq_3. The red-shift is likely due to the presence of the underlying thin silver film.

spectrums. Devices with F_{20}TPP:CBP (4:1) antennas had the highest PL efficiency and the greatest increase in external quantum efficiency. As shown in Fig. 4-6, quantum efficiencies were found to be 700% higher in devices utilizing these antennas relative to devices with non-functioning antennas in which the PL had been quenched by doping with CuPc.

4.5 Calculation of Energy Transfer Efficiency

The increase in external quantum efficiency, EQE , originates in sequential completion of three processes:

$$\eta_{EQE} = \eta_{ABS}^{Antenna} \times \eta_{Antenna-RC} \times \eta_{IQE}$$

where $\eta_{ABS}^{Antenna}$ is the normalized absorption in the antenna layer, $\eta_{Antenna-RC}$ is the energy transfer efficiency across the silver electrode, and η_{IQE} is the internal quantum efficiency of the organic PV.

For the devices with Alq_3 antennas the peak absorption in the antenna layer,

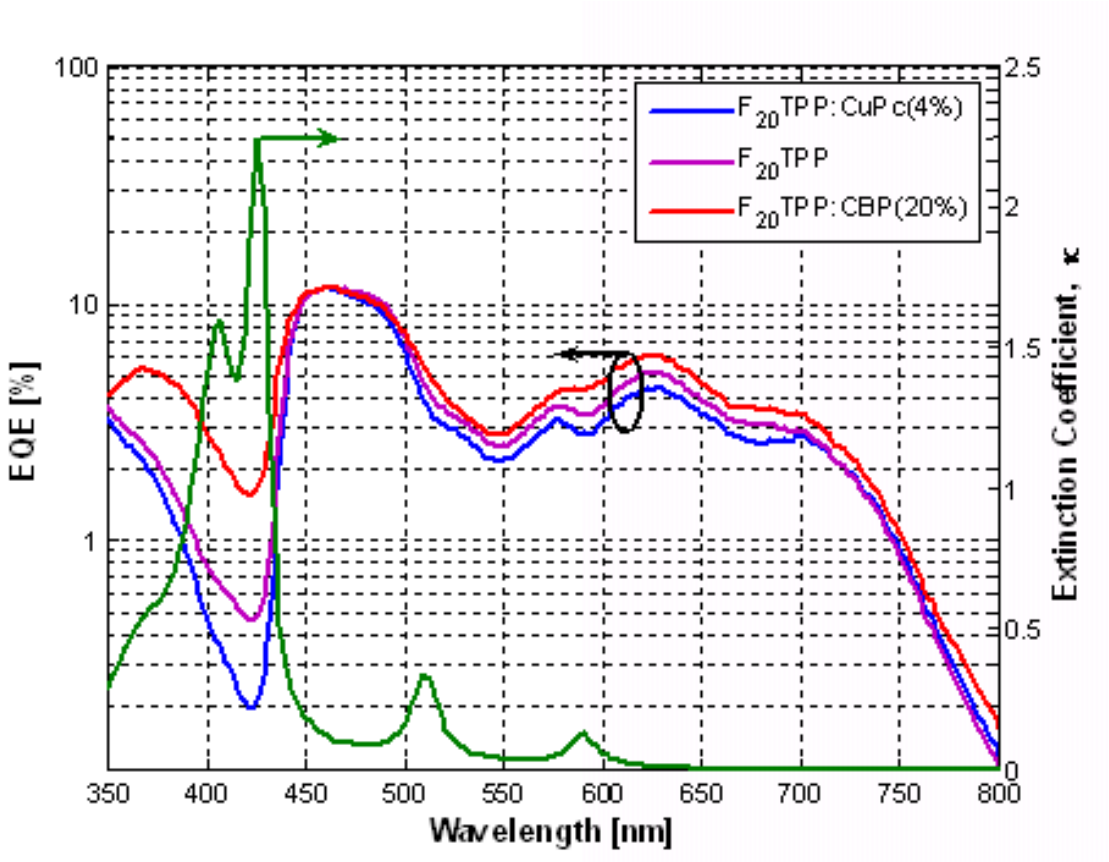

Figure 4-5: **F_{20}TPP antenna external quantum efficiency enhancement** External quantum efficiency scales with antenna PL efficiency in the range of wavelengths where F_{20}TPP has a non-zero extinction coefficient. In this region light is being absorbed in the antenna and transferred to the internal PV layers.

$\eta_{ABS}^{Antenna}$, was found to be 24% for all antenna compositions. Reflection and transmission measurements were taken to calculate total absorption in the active layers of the device with Alq3:CuPc antenna at $\lambda = 615$nm, the measured fluorescence maximum of DCM. From these measurements, η_{IQE} was found to be 5%. The total energy coupling efficiency across the silver film was found to be $\eta_{Antenna-RC} = 46\%$, similar to the predicted value of 52%. The overall gain in η_{EQE} was limited by low absorption in the antenna layer and relatively small η_{IQE} in this PV structure.

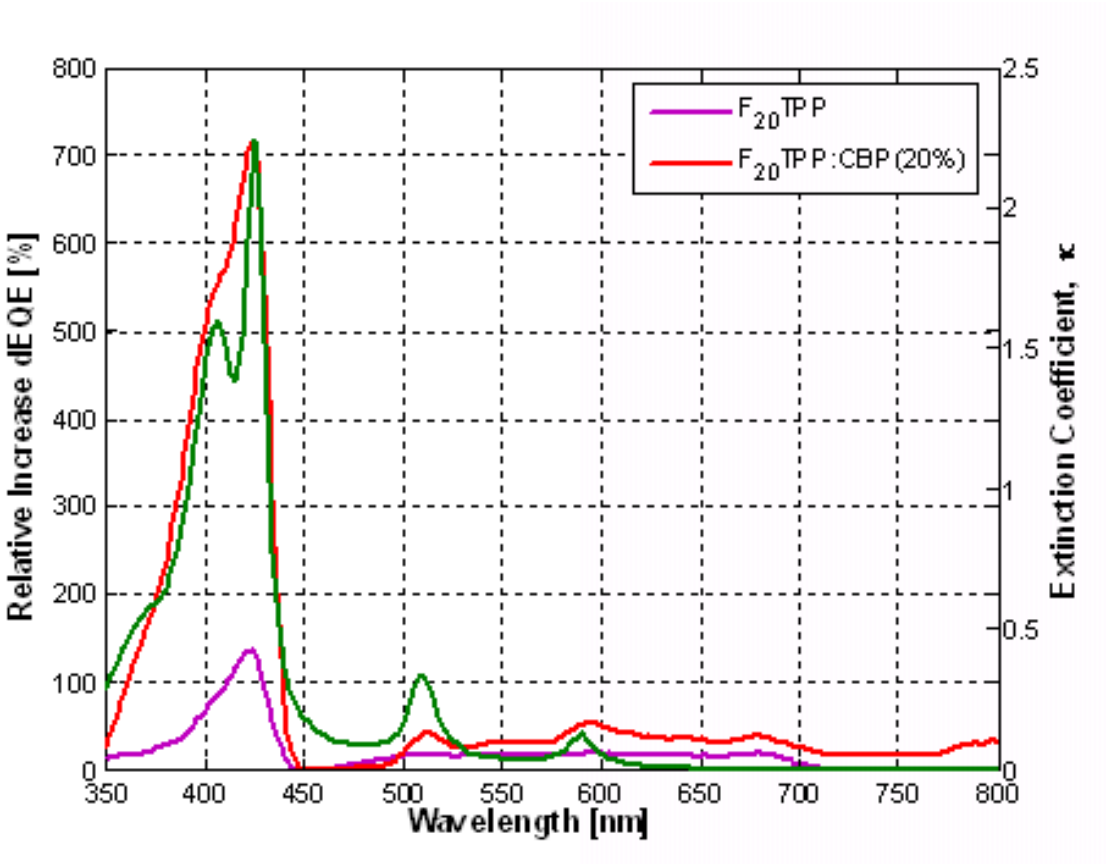

Figure 4-6: **F_{20}TPP antennas relative increase in external quantum efficiency** Devices with an antenna comprised of F_{20}TPP doped with CBP at a ratio of 4:1 result in a 700% increase in photocurrent relative to devices with non-functioning CuPc doped F_{20}TPP antennas. Antennas comprised of neat films of F_{20}TPP give a 100% increase in photocurrent.

Chapter 5

Conclusion

In this thesis I have proposed and demonstrated a novel new device architecture for organic photovoltaic devices inspired by the highly evolved architecture utilized in the process of photosynthesis to capture the sun's energy in nature. The device architecture consists of an external light absorbing antenna fabricated on top of an organic photovoltaic cell.

The tradeoff between light absorption and charge generation efficiency has been the focus of a great deal of research effort and many new architectures have been proposed previously including bulk heterojunction devices and tandem/stacked cells. While many of these previous efforts have achieved success in demonstrating higher efficiency devices, most have simply changed the constraints on the designer of organic PV instead of reduced the number of constraints. Tandem cells for example eliminate some of the problems with absorption by allowing greater total device thickness. However, new complications arise in ensuring each individual heterojunction produces the same magnitude of current. This constraint will no doubt lead to new tradeoffs and limitations in the design of these cells.

The addition of an external antenna is unique in that it separates the optical components of the cell from the electrical functions. Using an external antenna, each of these functions can be optimized separately. Highly absorptive antennas can be designed free of charge transport concerns while thin PV cells with near unity internal quantum efficiency can be designed independent of the need to absorb strongly across

the entire solar spectrum.

The true benefit of this approach will likely come by combining a highly efficient antenna with a thin PV charge separation cell optimized for the photoluminescence peak of the antenna. The breadth of materials available for use in optical antennas is far wider than those that have satisfactory characteristics for use in heterojunction charge separating cells. J-Aggregate materials, bio-materials, organic light emitting diode materials, and even quantum dots could all be used as antenna materials.

Another benefit of this approach is the use of two silver electrodes without the use of indium tin oxide (ITO). ITO is a transparent electrode material often employed in organic photovoltaic cells and light emitting diodes. ITO has also found heavy use in the production of liquid crystal displays. However, as demand has increased, the market price for ITO has risen dramatically. As the cost of ITO continues to rise, the use of ITO electrodes alone may price photovoltaics out of market competitiveness. Alternatives to using ITO electrodes such as that proposed here may become attractive. Transferring energy across semi-transparent or opaque electrodes via coupling with surface plasmon polariton could prove fundamental in these efforts.

Initial work on two very different antenna systems has been discussed. Antennas comprised of Alq_3 with high PL efficiency exhibited high energy transfer efficiency of approximately 50% while strongly absorbing $F_{20}TPP$ antennas exhibited increases in photocurrent as high as 700% when compared with devices with non-functioning antennas even with very low photoluminesence efficiencies near 4%.

Additional work is needed to find antennas exhibiting both strong absorption and high photoluminecence efficiency. Through blending materials in guest-host systems there is no reason this cannot be achieved. When coupled with optimized thin PV cells, it is likely that external antennas will be an additional architecture that can be used to increase power conversion efficiencies in organic photovoltaic devices.

Bibliography

[1] S. R. Bull. Renewable energy today and tomorrow. *Proceedings of the IEEE*, 89(8):1216–1226, 2001.

[2] S. G. Bailey and D. J. Flood. Space photovoltaics. *Progress in Photovoltaics: Research and Applications*, 6:1–14, 1998.

[3] E. Lorenzo. Photovoltaic rural electrification. *Progress in Photovoltaics: Research and Applications*, 5:3–27, 1997.

[4] A. Goetzberger and C. Hebling. Photovoltaic materials, past, present, future. *Solar Energy Materials & Solar Cells*, 62:1–19, 2000.

[5] J. Zhao, A. Wang, M.A. Green, and F. Ferrazza. Novel 19.8% efficient 'honeycomb' textured multicrystalline and 24.4% monocrystalline silicon solar cells. *Applied Physics Letters*, 73:1991–1993, 1998.

[6] J Meier, J. Sitznagel, U Kroll, C. Bucher, S. Fay, T. Moriarty, and A. Shah. Potential of amorphous and microcrystalline silicon solar cells. *Thin Solid Films*, 451-452:518–524, 2004.

[7] M.A. Green, E. Keith, D.L. King, Y. Hishikawa, and W. Warta. Solar cell efficiency tables (version 28). *Progress in Photovoltaics: Research and Applications*, 14:455–461, 2006.

[8] J. Xue, S. Uchida, B.P. Rand, and S.R. Forrest. Asymmetric tandem organic photovoltaic cells with hybrid planar-mixed molecular heterojunctions. *Applied Physics Letters*, 85(23):5757–5759, 2004.

[9] G. A. Chamberlain. Organic solar cells: A review. *Solar Cells*, 8(1):47–83, 1983.

[10] A. K. Ghosh, D. L. Morel, et al. Photovoltaic and rectification properties of al/mg phthalocyanine/ag schottky-barrier cells. *Journal of Applied Physics*, 45(1):230–236, 1974.

[11] C. W. Tang. Two-layer organic photovoltaic cell. *Applied Physics Letters*, 48(2):183–185, 1986.

[12] P. Würfel. *Physics of Solar Cells*, volume 2. Wiley-VCH, Weinheim, 2005.

[13] P. Peumans, A. Yakimov, and S. R. Forrest. Small molecular weight organic thin-film photodetectors and solar cells. *Journal of Applied Physics*, 93(7):3693–3723, 2003.

[14] M. Pope and C. Swenberg. *Electronic Processes in Organic Crystals*. Oxford University, Oxford, first edition, 1982.

[15] G. Zerza, C. J. Brabec, et al. Ultrafast charge transfer in conjugated polymer-fullerene composites. *Synthetic Metals*, 119(1-3):637–638, 2001.

[16] G. Yu and A. J. Heeger. Charge separation and photovoltaic conversion in polymer composites with internal donor-acceptor heterojunctions. *Journal of Applied Physics*, 78(7):4510–4515, 1995.

[17] J.J.M. Halls, C.A. Walsh, N.C. Greenham, E.A. Marseglia, R.H. Friend, S.C. Moratti, and A.B. Holmes. Efficient photodiodes from interpenetrating polymer networks. *Nature*, 376:498–500, 1995.

[18] S.E. Shaheen, C.J. Brabec, N.S. Sariciftci, F. Padinger, T. Fromherz, and J.C. Hummelen. 2.5% efficiency organic plastic solar cells. *Applied Physics Letters*, 78(6):841–843, 2001.

[19] P. Peumans, S. Uchida, and S.R. Forrest. Efficient bulk heterojunction photovoltaic cells using small-molecular-weight organic thin films. *Nature*, 425:158–162, 2003.

[20] A.K. Pandey, K.N.N. Unni, and J.M. Nunzi. Pentacene/perylene co-deposited solar cells. *Thin Solid Films*, 511-512:529–532, 2006.

[21] J. Xue, B.P. Rand, S. Uchida, and S.R. Forrest. Mixed donor-acceptor molecular heterojunctions for photovoltaic applications. ii. device performance. *Journal of Applied Physics*, 98(12), 2005.

[22] B.P. Rand, J. Xue, S. Uchida, and S.R. Forrest. Mixed donor-acceptor molecular heterojunctions for photovoltaic applications. i. material properties. *Journal of Applied Physics*, 98(12), 2005.

[23] B. Maennig, J. Drechsel, D. Gebeyehu, et al. Organic p-i-n solar cells. *Applied Physics A*, 79:1–14, 2004.

[24] M. Gratzel. Photoelectrochemicalcells. *Nature*, 414:338–344, 2001.

[25] M. Gratzel. Dye-sensitized solid-state heterojunction solar cells. *MRS Bulletin*, 30:23–27, 2005.

[26] J.R. Durrant and S.A. Haque. Solar cells: A solid compromise. *Nature Materials*, 2:362–363, 2003.

[27] W.U. Huynh, J.J. Dittmer, and A.P. Alivisatos. Hybrid nanorod-polymer solar cells. *Science*, 295:2425–2427, 2002.

[28] M. Law, L.E. Greene, J.C. Johnson, R. Saykally, and P. Yang. Nanowire dye-sensitized solar cells. *Nature Materials*, 4:455–459, 2005.

[29] A. Yakimov and S.R. Forrest. High photovoltage multiple-heterojunction organic solar cells incorporating interfacial metallic nanoclusters. *Applied Physics Letters*, 80(9):1667–1669, 2002.

[30] V. Shrotriya, E.H. Wu, Y. Yao, and Y. Yang. Efficient light harvesting in multiple-device stacked structure for polymer solar cells. *Applied Physics Letters*, 88(064104), 2006.

[31] L.A.A. Pettersson, L.S. Roman, and O. Inganäs. Enhanced photo conversion efficiency utilizing interference inside organic heterojunction photovoltaic devices. *Journal of Applied Physics*, 86(1):487–496, 1999.

[32] T Stũbinger and W. Brütting. Exciton diffusion and optical interference in organic donor-acceptor photovoltaic cells. *Journal of Applied Physics*, 90(7):3632–3641, 2001.

[33] L.S. Roman, O. Inganäs, T. Granlund, T. Nyberg, M. Svensson, M.R. Andersson, and J.C. Hummelen. Trapping light in polymer photodiodes with soft embossed gratings. *Advanced Materials*, 12(3):189–195, 2000.

[34] M. Niggemann, M. Glatthaar, A. Gombert, A. Hinsch, and V. Wittwer. Diffraction gratings and buried nano-electrodes-architectures for organic solar cells. *Thin Solid Films*, 451-452:619–623, 2004.

[35] M. Niggemann, M. Glatthaar, P. Lewer, C. Müller, J. Wagner, and A. Gombert. Functional microprism substrate for organic solar cells. *Thin Solid Films*, 511-512:628–633, 2006.

[36] M. Ihara, K. Tanaka, K. Sakaki, I. Homma, and K. Yamada. Enhanement of the absorption coefficient of *cis*-$(ncs)_2$ bis*2,2'-bipyridyl-4,4'-dicarboxylate)ruthenium(ii) dye in dye-sensitized solar cells by a silver island film. *Journal of Physical Chemistry B*, 101:5153–5157, 1997.

[37] B.P. Rand, P. Peumans, and S.R. Forrest. Long-range absorption enhancement in organic tandem thin-film solar cells containing silver nanoclusters. *Journal of Applied Physics*, 96(12):7519–7526, 2004.

[38] L.A.A. Pettersson, L.S. Roman, and O. Inganäs. Modeling photocurrent action spectra of photovoltaic devices based on organic thin films. *Journal of Applied Physics*, 86(1):487–496, 1999.

[39] O. Stenzel, A. Stendal, K. Voigtsberger, and C. von Borczyskowski. Enhancement of the photovoltaic conversion efficiency of copper phthalocyanine thin film

devices by incorporation of metal clusters. *Solar Energy Materials and Solar Cells*, 37:337–348, 1995.

[40] M. Westphalen, U. Kreibig, J. Rostalski, H. L*ddotu*th, and D. Meissner. Metal cluster enhanced organic solar cells. *Solar Energy Materials and Solar Cells*, 61(1):97–105, 2000.

[41] W.K. Purves. *Life, the science of biology*. Sunauer Associates, Inc.; W.H. Freeman and Co., Sunderland, MA; Gordonsville, VA, seventh edition, 2004.

[42] Jonathan K. Mapel. The application of photosynthetic materials and architectures to solar cells. Master's thesis, Massachusetts Institute of Technology, Electrical Engineering and Computer Science, 2006.

[43] H. Raether. *Surface Plasmons on Smooth and Rough Surfaces and on Gratings*, volume 111 of *Springer Tracts in Modern Physics*. Springer-Verlag, 1998.

[44] K. Welford. Surface-plasmon polaritons and their uses. *Optical and Quantum Electronics*, 23(1):1–27, 1991.

[45] J.M. Pitarke, V.M. Silkin, E.V. Chulkov, and P.M. Echenique. Surface plasmons in metallic structures. *Journal of Optics A: Pure and Applied Optics*, 7:S73–S84, 2005.

[46] T. Fuhrmann, K. Samse, J. Salbeck, A. Perschke, and H. Franke. Guided electromagnetic waves in organic light emitting diode structures. *Organic Electronics*, 4:219–226, 2003.

[47] T. Meumann, M.L. Johansson, D. Kambhampati, and W. Knoll. Surface-plasmon fluorescence spectroscopy. *Advanced Functional Materials*, 12(9):575–586, 2002.

[48] K.H. Yoon and M.L. Schuler. Design optimization of nano-grating surface plasmon resonance sensors. *Optics Express*, 14(11):4842–4849, 2006.

[49] T. Kume, S. Hayashi, and K. Yamamoto. Enhancement of photoelectric conversion efficiency in copper phthalocyanine solar cell by surface plasmon excitation. *Japanese Journal of Applied Physics*, 32(8):3486–3492, 1993.

[50] T. Wahamatsu, K. Saito, Y. Sakakibara, and H. Yokoyama. Surface plasmon-enhanced photocurrent in organic photoelectric cells. *Japanese Journal of Applied Physics*, 36(1A):155–158, 1997.

[51] E. Kretschmann and H. Raether. Radiative decay of non-radiative surface plasmons excited by light. *Zeitschrift für Naturforschung*, 23A:2135–2136, 1968.

[52] J.R. Sambles, G.W. Bradbery, and F. Yang. Optical excitation of surface plasmons: an introduction. *Contemporary Physics*, 32(3):173–183, 1991.

[53] R.R. Chance, A. Prock, and R. Silbey. Molecular fluorescence and energy transfer near interfaces. *Advances in Chemical Physics*, 37(1), 1978.

[54] G.J. Kovacs and G.S. Scott. Optical excitation of surface plasma waves in layered media. *Physical Review B*, 16(4):1297–1311, 1977.

[55] D.H. Drexhage. In E. Wolf, editor, *Progress in Optics XII*. North-Holland, New York, 1974.

[56] W.L. Barnes. Fluorescence near interfaces: the role of photonic mode density. *Journal of Modern Optics*, 45:661–699, 1998.

[57] W.H. Weber and C.F. Eagen. Energy transfer from an excited dye molecule to the surface plasmons of an adjacent metal. *Optics Letters*, 4(8):236–238, 1979.

[58] P. Andrew and W.L. Barnes. Energy transfer across a metal film mediated by surface plasmon polaritons. *Science*, 306:1002–1005, 2004.

[59] K. Celebi. unpublished.

[60] H. Mattoussi, H. Murata, C.D. Merritt, et al. Photoluminescence quantum yield of pure and molecularly doped organic solid films. *Journal of Applied Physics*, 86(5):2642–2650, 1999.